INDUCTION MOTOR DTC PERFORMANCE IMPROVEMENT BY REDUCING TORQUE RIPPLES IN LOW SPEED

Yassine Zahraoui[1], Mohamed Akherraz[2], Chaymae Fahassa[3]

The conventional direct torque control of an induction motor may provide satisfactory dynamic response. However, the conventional technique does not provide efficient dynamic performance during low speed or sudden changes in the load. To improve dynamic performance of the induction motor drive, a zone shifting technique is established on the conventional DTC in order to increase the fundamental value of inverter output voltage. Zone shifting DTC provides lesser current total harmonic distortion, flux distortion and torque pulsation compared to conventional DTC. All simulations have been realized in MATLAB/Simulink.

Keywords: modified DTC, zone shifting, low speed, induction motor drive, current total harmonic distortion, flux distortion, torque pulsation, speed sensorless, speed and flux observation, adaptive fuzzy Luenberger observer

Nomenclature

$i_{s\alpha}, i_{s\beta}$	$\alpha - \beta$ stator current components
$\phi_{r\alpha}, \phi_{r\beta}$	$\alpha - \beta$ rotor flux components
$u_{s\alpha}, u_{s\beta}$	$\alpha - \beta$ stator voltage components
T_r	Rotor time constant
Ω, ω_r	Rotor mechanical, electrical speed
ω_s, ω_{sl}	Stator, slip frequency
p	Number of pole pairs
C_s	Electromagnetic torque
R_s, R_r	Stator, rotor resistance
L_s, L_r, L_m	Stator, rotor, mutual inductance
σ	Leakage coefficient

[1]PhD student, Mohammed 5 University, Mohammadia School of Engineering, Morocco, e-mail: zahraoui.yassin@gmail.com

[2]Prof., Mohammed 5 University, Mohammadia School of Engineering, Morocco, e-mail: akherraz@emi.ac.ma

[3]PhD student, Mohammed 5 University, Mohammadia School of Engineering, Morocco, e-mail: fahassa.chaymae@gmail.com

1. Introduction

Induction motors (IM) are the most commonly and widely used electrical machines in several industrial applications; they are cheaper, rugged and easier to maintain comparing to other alternatives. But, their control is complex because of their nonlinear structure [1]; accordingly, the main objective of the IM control is to provide an efficient performance in a simple structure and the direct torque control (DTC) achieves this compromise [2]. The fundamental optimization of a drive system consists in obtaining the smallest overshoot in the shortest time of rising and settling at the speed level, and a high resistance to disturbances such as sudden load torque [3] [4].

The DTC structure of the IM drives was introduced in 1985 by I. Takahashi [5] and developed by M. Depenbrock [6], then, several studies made it possible to develop exactly the knowledge of this type of control. The DTC of an IM is based on the direct determination of the control sequence applied to the switches of a voltage inverter [8], this choice is generally based on the use of hysteresis regulators whose function is to control the state of the system, namely here the amplitude of the stator flux and the electromagnetic torque [9]. This type of control is classified in the category of amplitude controls, as opposed to the more conventional time control laws which are based on an adjustment of the average value of the pulse width modulation (PWM) vector [10].

DTC technique offers a fast response torque and flux control while avoiding the vector control complexity, as it requires a minimum number of controllers, and it does require neither voltage decoupling circuits nor coordinate transformation [11]. Despite these advantages, the conventional DTC control has some disadvantages; such as high ripples of the torque, flux and current, in addition to the slow transient response to the step changes in torque during start-up [12]. Further, the use of the speed sensor increases the complexity of the system, which is represented by additional cost, location problems and heavy volume addition. To improve the DTC control, there are several types of conventional DTC enhancement presented in the literature, zone shifting is one approach among them and it is effective especially in low speed [13].

Over the last few years, the sensorless speed control of IM drive has received a great interest. Thus, it is necessary to eliminate the speed sensor in order to reduce hardware and increase mechanical robustness. The main techniques of sensorless control of IM drive are: model reference adaptive systems (MRAS), extended Kalman filter (EKF) and adaptive Luenberger observer (ALO). Speed sensorless control methods of IM drive using the observed speed instead of the measured one have been studied in detail. In this paper, the

speed is observed from the instantaneous values of stator currents and voltages using the IM dynamic model in stator reference frame [14].

2. IM drive modeling

The mathematical model of a three-phase squirrel cage IM drive in $\alpha-\beta$ reference frame is:

$$\begin{cases} \dot{x} = \mathbf{A}.x + \mathbf{B}.u \\ y = \mathbf{C}.x \end{cases} \tag{1}$$

Where x, u and y are the state vector, the input vector and the output vector respectively.
$x = [i_{s\alpha}\ i_{s\beta}\ \phi_{r\alpha}\ \phi_{r\beta}]^t$; $u = [u_{s\alpha}\ u_{s\beta}]^t$; $y = [i_{s\alpha}\ i_{s\beta}]^t$

$$\mathbf{A} = \begin{bmatrix} -\lambda & 0 & \frac{K}{T_r} & K\omega_r \\ 0 & -\lambda & -K\omega_r & \frac{K}{T_r} \\ \frac{L_m}{T_r} & 0 & -\frac{1}{T_r} & -\omega_r \\ 0 & \frac{L_m}{T_r} & \omega_r & -\frac{1}{T_r} \end{bmatrix} \mathbf{B} = \begin{bmatrix} \frac{1}{\sigma L_s} & 0 \\ 0 & \frac{1}{\sigma L_s} \\ 0 & 0 \\ 0 & 0 \end{bmatrix} \mathbf{C} = \begin{bmatrix} 1 & 0 & 0 & 0 \\ 0 & 1 & 0 & 0 \end{bmatrix}$$

With: $\lambda = \frac{R_s}{\sigma.L_s} + \frac{1-\sigma}{\sigma.T_r}$; $K = \frac{1-\sigma}{\sigma.L_m}$; $\sigma = 1 - \frac{L_m^2}{L_s.L_r}$; $T_r = \frac{L_r}{R_r}$

Figure 1 shows the state space mathematical model of the IM drive and Table 1 lists its rated power and parameters.

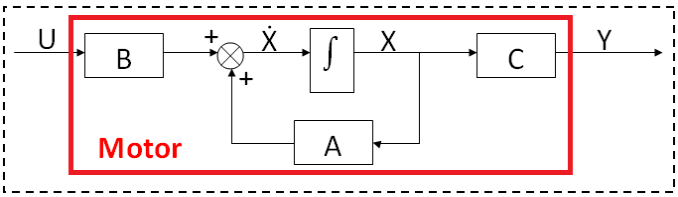

FIGURE 1. State space mathematical model of the IM drive

TABLE 1. IM drive rated power and parameters

Rated power	3 kW
Pair pole	2
Rated speed	1440 rpm
Stator resistance	2.2 Ω
Rotor resistance	2.68 Ω
Stator inductance	0.229 H
Rotor inductance	0.229 H
Mutual inductance	0.217 H
Moment of inertia	0.047 $kg.m^2$
Viscous friction coefficient	0.004 N.s/rad

3. DTC Basis

The conventional DTC of an IM drive allows the control of the flux and torque directly and independently through selecting the optimal inverter switching modes, while maintaining the flux and torque within their hysteresis bands respectively. Thus, the DTC provides a very fast torque response without using coordinate transformation, current regulators and PWM generator.

3.1. Stator Flux and Torque Estimation

The torque and flux are calculated based on the stator current and voltage measurements through an estimator. On the basis of the IM drive dynamic model in the stator reference frame, the stator flux equation is [7]:

$$\bar{\phi_s} = \int_0^t (\bar{V_s} - R_s \bar{I_s}) dt \tag{2}$$

The flux components in the (α, β) coordinates are:

$$\phi_{s\alpha} = \int_0^t (V_{s\alpha} - R_s I_{s\alpha}) dt \tag{3}$$

$$\phi_{s\beta} = \int_0^t (V_{s\beta} - R_s I_{s\beta}) dt \tag{4}$$

The stator flux module is written as:

$$\phi_s = \sqrt{\phi_{s\alpha}^2 + \phi_{s\beta}^2} \tag{5}$$

The torque equation is:

$$T_s = \frac{3}{2} p (I_{s\beta} \phi_{s\alpha} - I_{s\alpha} \phi_{s\beta}) \tag{6}$$

3.2. Switching state vector

When compared to their reference values, the estimated values provide errors which are the inputs to the hysteresis controllers. These controller outputs along with the flux location are the selector table inputs, whereas its output is the suitable switching states vector (Table 2).

Table 2. Optimal switching mode table

$\Delta\phi_s$	ΔC_s	S1	S2	S3	S4	S5	S6
1	1	110	010	011	001	101	100
	0	111	000	111	000	111	000
	-1	101	100	110	010	011	001
0	1	010	011	001	101	100	110
	0	000	111	000	111	000	111
	-1	001	101	100	110	010	011

This switching states vector (S_a S_b S_c) generates eight position vectors ($\vec{V}_1, \vec{V}_2, ..., \vec{V}_8$), where two of them correspond to the null vector (S_a S_b S_c)=(1 1 1) or (0 0 0) as shown in Figure 2.

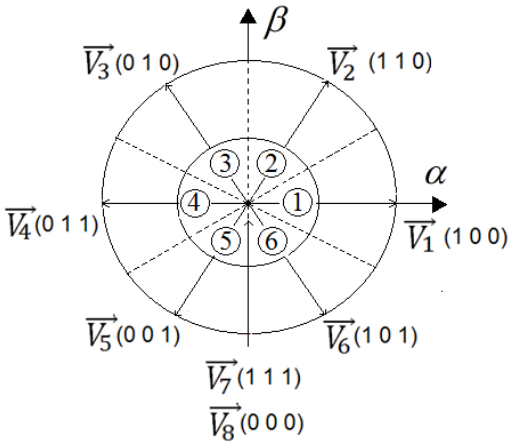

FIGURE 2. Stator voltage vectors

Figure 3 shows the overall structure of the proposed sensorless DTC.

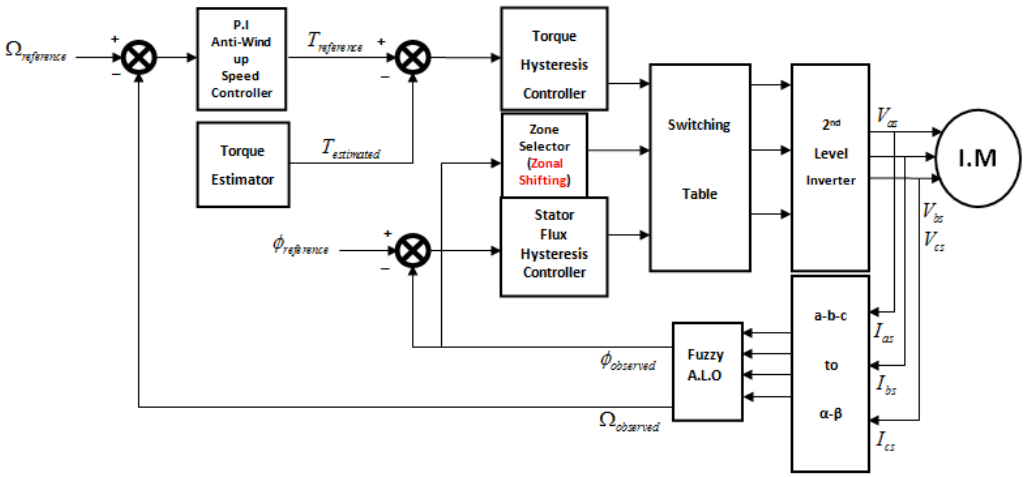

FIGURE 3. The overall structure of the proposed control

3.3. PI Anti-Windup Controller

The structure of the PI anti-windup controller based on the back calculation method is presented in Figure 4. The saturation error u_e and anti-windup gain K_s are the main parameters for the integral action correction, where:

$$u_e = u_{in} - u_{out} \tag{7}$$

u_{in} and u_{out} are the input and the output of the saturation component respectively.

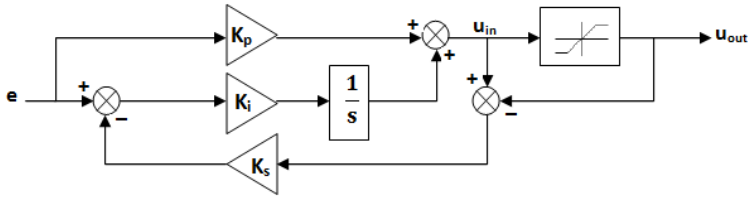

FIGURE 4. PI anti-windup based on back calculation method

3.4. **Zone shifting technique**

There are many techniques that are used to improve the conventional DTC, especially in terms of the reduction of the electromagnetic torque and the stator flux ripple and to control the variation of the switching frequency. Zone shifting strategy is one among them and is based on a zone shifting of the conventional DTC by changing the switching table and changing the zones. Instead of taking the first sector from $-30°$ to $+30°$, it should be taken from $0°$ to $+60°$ which characterize a new partition of the zones as defined in the Figure 5. This type of control allows a good operation performance especially at low speed [8].

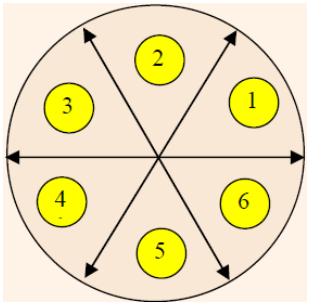

FIGURE 5. New partition of the zones

4. **Adaptive Luenberger observer for rotor flux and speed estimation**

The Adaptive flux observer is a deterministic type of observers based on a deterministic model of the system [3]. In this work, the adaptive Luenberger state observer (ALO) is used to estimate the flux components and rotor speed of the IM drive by including an adaptive mechanism based on the Lyapunov

theory and fuzzy regulation. In general, the equations of the ALO can be expressed as follow:

$$\begin{cases} \dot{\hat{x}} = \mathbf{A}.\hat{x} + \mathbf{B}.u + \mathbf{L}.(y - \hat{y}) \\ \hat{y} = \mathbf{C}.\hat{x} \end{cases} \tag{8}$$

The symbol $\hat{}$ denotes the estimated value and $\mathbf{L}$ is the observer gain matrix. The mechanism of adaptation speed is deduced by Lyapunov theory. The estimation error of the stator current and rotor flux, which is the difference between the observer and the model of the motor, is given by:

$$\dot{e} = (\mathbf{A} - \mathbf{L}.\mathbf{C}).e + \Delta\mathbf{A}.\hat{x} \tag{9}$$

Where

$$e = x - \hat{x} \tag{10}$$

$$\Delta\mathbf{A} = \mathbf{A} - \tilde{\mathbf{A}} = \begin{bmatrix} 0 & 0 & 0 & K.\Delta\omega_r \\ 0 & 0 & -K.\Delta\omega_r & 0 \\ 0 & 0 & 0 & -\Delta\omega_r \\ 0 & 0 & \Delta\omega_r & 0 \end{bmatrix} \tag{11}$$

$$\Delta\omega_r = \omega_r - \hat{\omega_r} \tag{12}$$

Definition 4.1. *We consider the following Lyapunov function:*

$$V = e^t.e + \frac{(\Delta\omega_r)^2}{\lambda} \tag{13}$$

Where λ is a positive coefficient, its derivative is given as follow:

$$\dot{V} = e^t[(\mathbf{A} - \mathbf{LC})^t + (\mathbf{A} - \mathbf{LC})]e - 2K\Delta\omega_r(e_{i_{s\alpha}}\hat{\phi_{r\beta}} - e_{i_{s\beta}}\hat{\phi_{r\alpha}}) + \frac{2}{\lambda}\Delta\omega_r\dot{\hat{\omega}}_r \tag{14}$$

With $\hat{\omega_r}$ is the estimated rotor speed. The adaptation law for the estimation of the rotor speed can be deduced by the equality between the second and third terms of Equation 14:

$$\hat{\omega_r} = \int \lambda.K.(e_{i_{s\alpha}}.\hat{\phi_{r\beta}} - e_{i_{s\beta}}.\hat{\phi_{r\alpha}}).dt \tag{15}$$

The feedback gain matrix $\mathbf{L}$ is chosen to ensure the fast and robust dynamic performance of the closed loop observer.

$$\mathbf{L} = \begin{bmatrix} l_1 & -l_2 \\ l_2 & l_1 \\ l_3 & -l_4 \\ l_4 & l_3 \end{bmatrix} \tag{16}$$

With l_1, l_2, l_3 and l_4 are given by:

$$l_1 = (k_1 - 1).(\gamma + \tfrac{1}{T_r}) \; ; \; l_2 = -(k_1 - 1).\hat{\omega_r}$$
$$l_3 = \tfrac{(k_1^2 - 1)}{K}.(\gamma - K.\tfrac{L_m}{T_r}) + \tfrac{(k_1 - 1)}{K}.(\gamma + \tfrac{1}{T_r}) \; ; \; l_4 = -\tfrac{(k_1 - 1)}{K}.\hat{\omega_r}$$

Remark 4.1. k_1 is a positive coefficient obtained by pole placement approach [3]; a wise choice was made for its value which is 1.06 in order to guarantee a fast response. Fuzzy logic control (FLC) in adaptation mechanism replaces conventional control [15] and it gives robust performance against parameter variation and machine saturation [16] [17]

The state space mathematical model of the adaptive observer is illustrated by Figure 6.

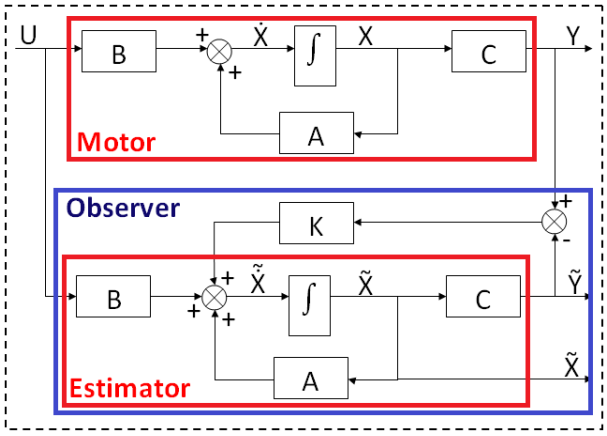

FIGURE 6. State space mathematical model of the adaptive observer

5. Simulation Results

A series of simulation tests were carried out on the proposed system. During all the tests, the reference of the stator flux is set to 1 Wb and a sudden load of 10 $N.m$ is applied at $0.5s$ and removed at $0.8s$ in order to test the system stability. A 20 rad/s step reference speed is applied at $0s$. The step reference is chosen because it is the hardest for most control processes.
There is an improvement in speed regulation with less flux distortion and torque pulsation even under the instant load conditions as shown in Figures 7 and 8. In Figures 9, 10 and 11, the steady state is reached quickly and the starting torque and currents reach maximum values and are stabilized at the same time, the starting torque is high in order to overcome the inertia and friction and the dynamics of speed is very fast with a short response time. This means the high performance of the flux and torque estimators, and the speed anti-windup regulator too.
The torque THD is reduced from 74.63% to 45.69% and the phase current THD is reduced from 57.89% to 40.45%. The switching frequency of the zone shifting technique is constant, the reason is that each inverters interrupter has a rest moment (switching off) which can reduce the commutation losses even in steady state or in transient operation.

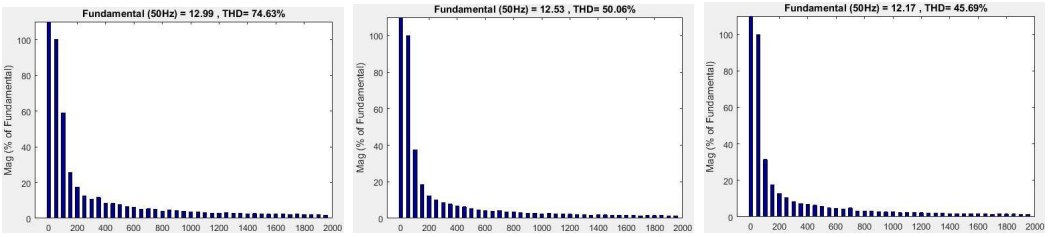

(A) THD at 0° shifting (B) THD at 15° shifting (C) THD at 30° shifting

FIGURE 7. Torque THD improvement

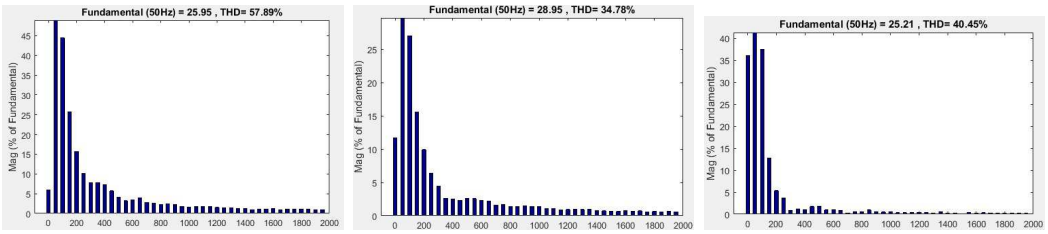

(A) THD at 0° shifting (B) THD at 15° shifting (C) THD at 30° shifting

FIGURE 8. Phase current THD improvement

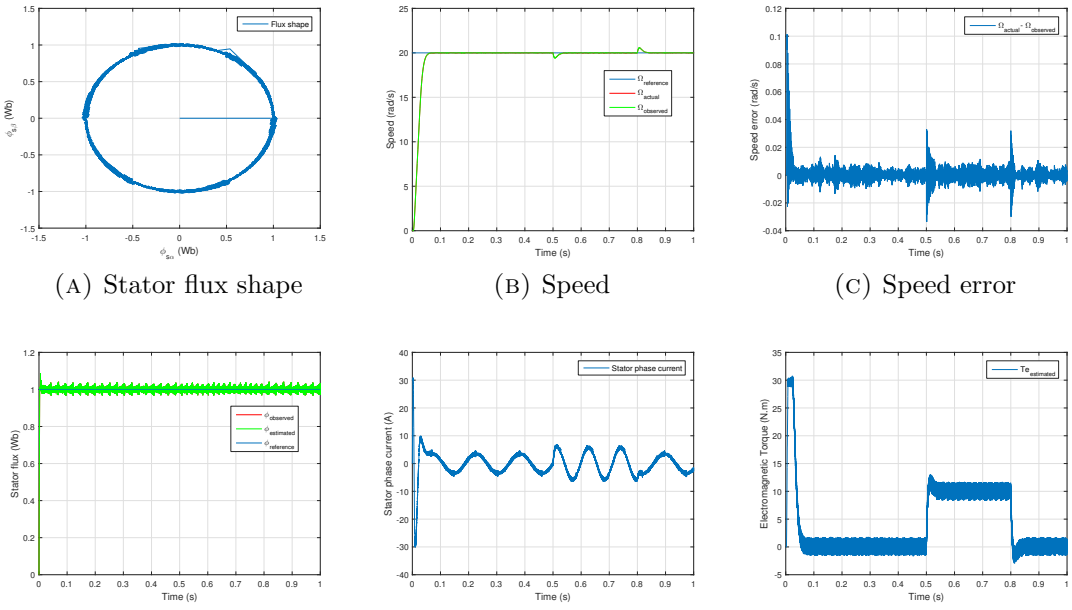

(A) Stator flux shape (B) Speed (C) Speed error

(D) Stator flux (E) Stator phase current (F) Torque

FIGURE 9. Operating at 0° zone shifting

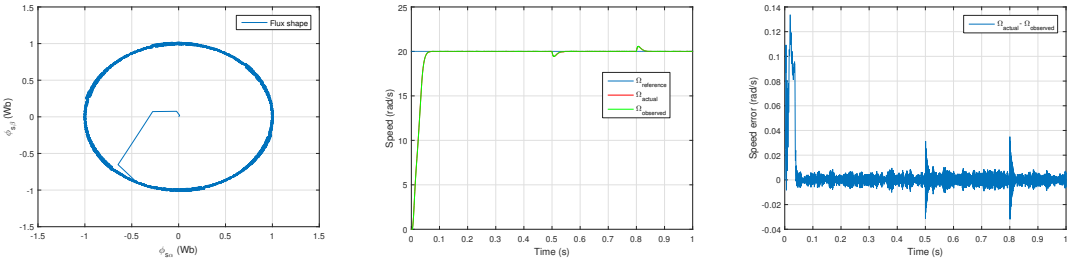

(A) Stator flux shape (B) Speed (C) Speed error

(D) Stator flux (E) Phase current (F) Torque

FIGURE 10. Operating at 15° zone shifting

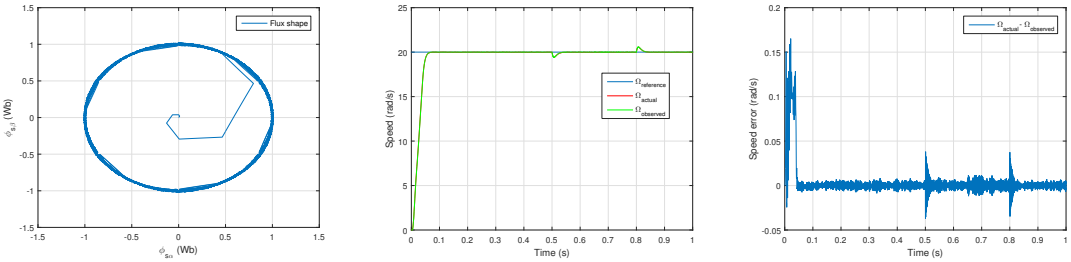

(A) Stator flux shape (B) Speed (C) Speed error

(D) Stator flux (E) Phase current (F) Torque

FIGURE 11. Operating at 30° zone shifting

6. Conclusion

Zone shifting DTC for a three-phase 3kW induction motor drive is simulated in the MATLAB/Simulink environment, and the dynamic performance is studied too. The starting current, speed regulation, flux distortion and torque pulsation are much lower with 30° zone shifting technique. The simulated responses show that the system performance during instant load is good, the simulated current and torque THD during the steady state are improved, with faster dynamic characteristic.

The constant switching frequency based DTC strategy has a reducer ripples level basing on zone shifting technique compared to the conventional DTC, where it is observed that the high torque ripples exceed the hysteresis boundary. The modified DTC shows a reducer flux ripples, faster magnitude tracking at the starting up and better components waveform than the conventional DTC.In conclusion, zone shifting technique has proved good performance dynamic for IM drive DTC control type especially at very low speed.

REFERENCES

[1] *R. Krishnan*, Electric Motor Drives: Modeling, Analysis, and Control, 1st ed. Upper Saddle River, N.J: Pearson, Feb. 2001.

[2] *B. K. Bose*, Modern Power Electronics and AC Drives, 1st ed. Upper Saddle River, NJ: Prentice Hall, Oct. 2001.

[3] *P. Vas*, Sensorless Vector and Direct Torque Control. Oxford University Press, 1998.

[4] *B. Wu and M. Narimani*, High-Power Converters and AC Drives. John Wiley and Sons, Jan. 2017.

[5] *I. Takahashi and T. Noguchi*, A New Quick-Response and High- Efficiency Control Strategy of an Induction Motor, IEEE Transactions on Industry Applications, vol. IA-22, no. 5, pp. 820827, Sep. 1986.

[6] *M. Depenbrock*, Direct self-control (DSC) of inverter-fed induction machine, IEEE Transactions on Power Electronics, vol. 3, no. 4, pp. 420429, Oct. 1988.

[7] *L. Laggoun, L. Youb, S. Belkacem, S. Benaggoune, A. Craciunescu*, Direct torque control using second order sliding mode of a double star permanent magnet synchronous machine, University Politehnica of Bucharest Scientific Bulletin Series C Electrical Engineering and Computer Science, vol. 80, no. 4, 2018.

[8] *V. Jose, K. V. Kumar, S. S. Kumar, N. T. Abraham, and D. M. Mathew*, Analysis of Direct Torque Control of Industrial Drives using Zone-Shifting SVM, International Journal of Power Electronics and Drive Systems (IJPEDS), vol. 4, no. 3, pp. 321328, Sep. 2014.

[9] *E. E. El-Kholy, S. Mahmoud, R. Kennel, A. El-Refaei, and F. Elkady*, Torque Ripple Minimization for Induction Motor Drives with Direct Torque Control, Electric Power Components and Systems, vol. 33, no. 8, pp. 845859, Aug. 2005.

[10] *S. Belkacem, F. Naceri, and R. Abdessemed*, Reduction of torque ripple in DTC for induction motor using input-output feedback linearization, 2012.

[11] *H. Ismail, F. Patkar, A. Jidin, A. Z. Jidin, N. A. N. Azlan, and T. Sutikno*, Constant Switching Frequency and Torque Ripple Minimization of DTC of Induction Motor

Drives with Three-level NPC Inverter, International Journal of Power Electronics and Drive Systems (IJPEDS), vol. 8, no. 3, pp. 10351049, Sep. 2017.

[12] *T. V. Kumar and S. S. Rao*, Reduction of torque ripple in direct torque control of induction motor using constant switching frequency operation, in 7th Mediterranean Conference and Exhibition on Power Generation, Transmission, Distribution and Energy Conversion (Med-Power 2010), Nov. 2010, pp. 16.

[13] *S. H., K. S.f., and S. B.*, Improvements in direct torque control of induction motor for wide range of speed operation using fuzzy logic, Journal of Electrical Systems and Information Technology, vol. 5, no. 3, pp. 813828, Dec. 2018.

[14] *Y. Zahraoui, C. Fahassa, M. Akherraz, and A. Bennassar*, Sensorless vector control of induction motor using an EKF and SVPWM algorithm, in 2016 5th International Conference on Multimedia Computing and Systems (ICMCS), Sep. 2016, pp. 588593.

[15] *L. A. Zadeh*, Fuzzy sets, Information and Control, vol. 8, no. 3, pp. 338353, Jun. 1965.

[16] *M. Y. Zidani, L. Youb, S. Belkacem, and F. Naceri*, Design of robust control using fuzzy logic controller for doubly-fed induction motor drives, University Politehnica of Bucharest Scientific Bulletin Series C Electrical Engineering and Computer Science, vol. 81, no. 1, pp. 159170, 2019.

[17] *B. Tahar, B. Bousmaha, B. Ismail, and B. Houcine*, Speed Sensorless Field-Oriented Control of Induction Motor with Fuzzy Luenberger Observer. Electrotehnica, Electronica, Automatica, vol. 66, no 4, p. 22, 2018.